Original research article

Syntrophy between fermentative and purple phototrophic bacteria for carbohydrate-based wastewater treatment

Marta Cerruti[1], Guillaume Crosset-Perrotin[1], Mythili Ananth[1], Jules L. Rombouts[1,2] and David G. Weissbrodt[1,*]

[1] Department of Biotechnology, Delft University of Technology, Delft, The Netherlands

[2] Nature's Principles B.V., Den Haag, The Netherlands

* Correspondence: Prof. David Weissbrodt, Weissbrodt Group for Environmental Life Science Engineering, Environmental Biotechnology Section, Department of Biotechnology, TNW Building 58, van der Maasweg 9, 2629 HZ Delft, The Netherlands, Tel: +31 15 27 81169; E-mail: d.g.weissbrodt@tudelft.nl

ABSTRACT

Fermentative chemoorganoheterotrophic bacteria (FCB) and purple photoorganoheterotrophic bacteria (PPB) are two interesting microbial guilds to process carbohydrate-rich wastewaters. Their interaction has been studied in axenic pure cultures or co-cultures. Little is known about their metabolic interactions in open cultures. We aimed to harness the competitive and syntrophic interactions between PPB and FCB in mixed cultures. We studied the effect of reactor regimes (batch or continuous, CSTR) and illumination modes (continuous irradiation with infrared light, dark, or light/dark diel cycles) on glucose conversions and the ecology of the process. In batch, FCB outcompeted (>80%) PPB, under both dark and infrared light conditions. In CSTR, three FCB populations of *Enterobacteriaceae*, *Lachnospiraceae* and *Clostridiaceae* were enriched (>70%), while *Rhodobacteraceae* relatives of PPB made 30% of the community. Fermentation products generated from glucose were linked to the dominant FCB. Continuous culturing at a dilution rate of 0.04 h^{-1} helped maintain FCB and PPB in syntrophy: FCB first fermented glucose into volatile fatty acids and alcohols, and PPB grew on fermentation products. Direct supply of carboxylates like acetate under infrared light enriched for PPB (60%) independent of reactor regimes. Ecological engineering of FCB- and PPB-based biorefineries can help treat and valorize carbohydrate-based waste feedstocks.

Keywords: photoorganoheterotrophs; chemoorganoheterotrophs; syntrophy; mixed-culture fermentation; resource recovery

38 **GRAPHICAL ABSTRACT**

39

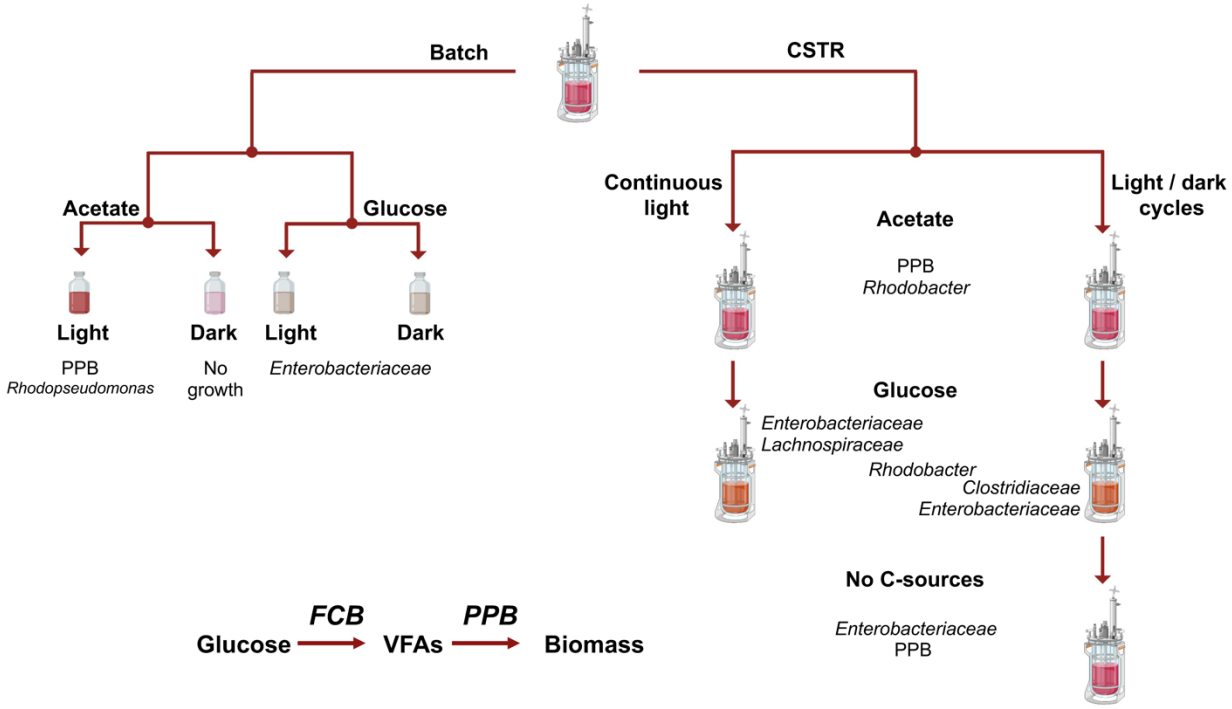

40

41

INTRODUCTION

In the natural environment, bacteria evolved to occupy diverse niches (Steindler et al., 2020). Microorganisms form metabolic associations to grow under nutrient-limiting conditions (Pearman et al., 2008). Anthropogenic environments like biological wastewater treatment plants (WWTPs) involve relatively high concentrations of organics (up to 200 g COD L^{-1}) and other nitrogenous and phosphorous nutrients, and complex compositions of carbon sources like cellulose and undigested fibers from food. In agri-food industrial wastewaters, most of organics are derived from simple carbohydrates (*e.g.*, glucose, fructose or xylose) and polymeric sugars such as starch, cellulose and lignocellulosic derivates (Ghosh et al., 2017).

The wastewater treatment sector transitions to develop bioprocesses that combine nutrient removal with bioproduct valorization. Environmental biotechnologies are studied to treat and valorize nutrient-rich wastewaters by unravelling the biochemical mechanisms that can drive product formation (Kleerebezem & van Loosdrecht, 2007). The efficiency of mixed-culture processes is based on proper selection of microbial guilds needed to metabolize the wastes. Two guilds across chemo- and photoorganoheterotrophic groups are particularly attractive to process carbohydrate- and carboxylate-based feedstocks.

Fermentative chemoorganoheterotrophic bacteria (FCB) degrade carbohydrates through fermentation pathways, producing a spectrum of valuable compounds such as carboxylates (*e.g.*, volatile fatty acids – VFAs, lactic acid), ethanol and H_2. Their microbial niches are harnessed in non-axenic mixed-culture fermentation processes to valorize, *e.g.*, lignocellulosic sugars into targeted fermentation products like lactate or ethanol (Rombouts et al., 2020).

Purple phototrophic bacteria (PPB) are versatile microorganisms, involving a diversity of phototrophic and chemotrophic metabolisms depending on environmental and physiological conditions (**Table 1**). They grow preferentially as photoorganoheterotrophs, harvesting their energy from infrared (IR) light and using a variety of carbon sources from carboxylates to carbohydrates to

alcohols (Imam et al., 2011; Okubo et al., 2005; D. Puyol et al., 2017). PPB can also grow as chemotrophs using organic or inorganic substrates (Hunter et al., 2009). As photoheterotrophs, they can achieve high biomass yields up to 1 g COD_X g^{-1} COD_S (Daniel Puyol & Batstone, 2017), that can be exploited to valorize anabolic products like biomass, single-cell proteins used in animal/human feed, or industrially relevant compounds like carotenoids.

Table 1. Metabolic versatility of purple phototrophic bacteria (PPB). PPB can grow by combining a diversity of substrates and redox conditions. PPB grow primarily as photoorganoheterotrophs using VFAs as preferential carbon sources. but they are able to grow also on glucose with low growth rates. The metabolisms targeted in this study for the conversion of glucose by combination of fermentation and photoorganoheterotrophy are highlighted in grey.

Metabolism	**Energy source** (photo-/chemo-)	**Electron donors** (organo-/litho-)	**Oxidized e-donors**	**Carbon source** (hetero-/auto-)	**Electron acceptors**	**Reduced e-acceptors**
Under light conditions						
Anoxygenic photoorganoheterotrophy	Light photons	Reduced organic	Oxidized organic, CO_2	Organic	Endogenous compound, CO_2 fixation	Biomass
Anoxygenic photolithoautotrophy	Light photons	Reduced inorganic H_2 H_2S Fe^{2+} NO_2^- H_2O	Oxidized inorganic H_2O SO_4^{2-} Fe^{3+} NO_3^- O_2	Inorganic (CO_2)	Endogenous compound, CO_2 fixation	Biomass
Oxygenic photolithoautotrophy	Light photons			Inorganic (CO_2)	Endogenous compound, CO_2 fixation	Biomass
Photofermentation (not growth associated)	Light photons	Excess electrons energized from substrate	-	-	H^+	H_2
Under dark conditions						
Aerobic-respiring chemoorganoheterotrophy	Chemical redox reaction by aerobic respiration	Reduced organic	CO_2	Organic	O_2	H_2O Biomass
Anaerobic-respiring chemoorganoheterotrophy	Chemical redox reaction by anaerobic respiration	Reduced organic	CO_2	Organic	NO_3^- SO_4^{2-}	N_2 S^0, HS^-, H_2S Biomass
Fermentative chemoorganoheterotrophy	Chemical redox reaction by fermentation	Reduced organic (*e.g.*, fermentable sugars)	Pyruvate or CO_2	Organic	Endogenous compound	Fermentation products (*e.g.*, acetate, H_2), Biomass

Further studies evaluated PPB ability to do photofermentation, coupling glucose degradation to H_2 production. Combinations of fermentative chemoorganoheterotrophy, photoorganoheterotrophy and photofermentation processes have been tested for carbohydrate degradation and conversion. In (*i*) *two-stage dark fermentation and photoorganoheterotrophy*, the process is carried in two separate reactors. In the first unit, pure cultures of FCB degrade carbohydrates into VFAs that are then fed in the second unit to produce PPB biomass in pure cultures (Ghimire et al., 2015). In (*ii*) *single-stage fermentation*, glucose is degraded by pure-cultures of PPB, with longer contact times compared to the two-stages fermentation and the requirement of a pre-sterilized feed stream and axenic environment (Abo-Hashesh & Hallenbeck, 2012). In (*iii*) *single-stage dark and photofermentation*, attempts have been made to co-cultivate defined species of FCB and PPB to simultaneously degrade carbohydrates and convert the produced VFAs to biomass (Rai & Singh, 2016). Despite the advantages of this technique, including lower investment and operation costs compared to the two-staged fermentation, it still requires an axenic environment.

In this context of associating fermentation and photoorganoheterotrophy, one can also wonder whether PPB, due to their metabolic versatility, could be selected in the mixed culture to perform both dark fermentation and photoorganoheterotrophy, or whether FCB would be more efficient on fermentation, prior to supplying fermentation products for the PPB to grow.

Open mixed cultures have the advantage, compared to traditional industrial biotechnology approaches, to not require sterilization of the inflow, therefore substantially reducing the costs (Kleerebezem & van Loosdrecht, 2007). Based on ecological selection principles, microorganisms can be selected to specifically target substrate degradation, bioproduct valorization or both.

Many studies have focused on H_2 production with FCB and PPB pure cultures or with co-cultures in axenic conditions. Little is known about the community dynamics in open mixed cultures. The interactions between populations and their metabolic interdependency have not been unraveled.

Here, we evaluated the ecological association of PPB and FCB in carbohydrate-fed mixed cultures. We addressed the selection mechanisms, competitive and syntrophic interactions of the two microbial guilds across reactor (batch, chemostat) and IR light irradiance (light, dark, dark/light) regimes using either glucose or acetate as model carbohydrate and carboxylate substrates that harbor the same degree of reduction (4 mol e^- C-mol^{-1}). With this microbial ecology insights, we tested the possibility to treat carbohydrate-rich wastewaters in a single-stage mixed-culture process assembling FCB and PPB in syntrophy.

MATERIAL AND METHODS

Mixed-culture bioreactor systems

To evaluate microbial competition between PPB and fermenters, two mixed-culture bioreactor regimes (batch and continuous culturing), two substrates with the same degree of reduction per carbon mole (acetate and glucose), and three light patterns (continuous illumination, continuous dark, and light / dark switches with a ratio of 12h / 8h) were applied. The reactor performances were measured by quantitative biotechnology endpoints (rates, yields). Microbial selection and community dynamics were tracked by 16S amplicon sequencing. The experimental design is shown in **Table 2**.

Table 2. Combinations of operational conditions tested to address selection, competition, and interaction mechanisms between FCB and PPB.

Reactor regime	Organic substrate	Illumination	Input concentration of organic matter (gCOD L^{-1})
Batch	Acetate	Continuous	10
Batch	Acetate	No (dark)	10
Batch	Glucose	Continuous	10
Batch	Glucose	No (dark)	10
CSTR	Acetate	Continuous	5 / 10
CSTR	Glucose	Continuous	5
CSTR	Acetate	16h light / 8h dark	10
CSTR	Glucose	16h light / 8h dark	10
CSTR	No carbon sources	16h light / 8h dark	-

Compositions of cultivation media

Under all conditions, the cultures were provided with a mineral medium composed of (per L): 0.14 g KH_2PO_4, 0.21 g K_2HPO_4, 1 g NH_4Cl, 2 g $MgSO_4 \cdot 7H_2O$, 1 g $CaCl_2 \cdot 2H_2O$, 1 g NaCl, and 2 mL of trace elements and 2 mL of vitamins solutions. The stock solution of vitamins was composed of 200 mg thiamine–HCl, 500 mg niacin, 300 mg ρ-amino-benzoic acid, 100 mg pyridoxine–HCl, 50 mg biotin and 50 mg vitamin B12 per liter. The trace elements solution was made of (per L): 1100 mg $Na_2EDTA \cdot 2\ H_2O$, 2000 mg $FeCl_3 \cdot 6\ H_2O$, 100 mg $ZnCl_2$, 64 mg $MnSO_4 \cdot H_2O$, 100 mg H_3BO_3, 100 mg $CoCl_2 \cdot 6\ H_2O$, 24 mg $Na_2MoO_4 \cdot 2\ H_2O$, 16 mg $CuSO_4 \cdot 5\ H_2O$, 10 mg $NiCl_2 \cdot 6\ H_2O$ and 5 mg $NaSeO_3$. The cultivation medium was buffered at pH 7.0 with 4 g L^{-1} 4-(2-hydroxyethyl)-1piperazineethanesulfonic acid (HEPES). Sodium acetate and glucose were used as carbon sources,

in a concentration of 5 or 10 g COD L^{-1} depending on experimental conditions (**Table 2**), mimicking concentrations of moderately loaded agri-food wastewaters. Acetate was provided as $C_2H_3O_2 \cdot 3H_2O$ (18.28 g L^{-1}) and glucose as $C_6H_{12}O_6 \cdot H_2O$ (9.68 g L^{-1}).

Batches operational conditions

PPB biomass from an in-house enrichment culture grown in a sequencing batch reactor (SBR) (Cerruti et al., 2020) was used to inoculate 100-ml anaerobic bottles. The cultures were flushed with 99% argon gas to maintain anaerobic conditions (Linde, NL, >99% purity). Every batch bottle was duplicated. Half of the batch bottles were exposed to dark. The other half were exposed to IR light (> 700 nm) supplied by a halogen lamp (white light) with a power of 120 W whose wavelengths below 700 nm were filtered out by two filter sheets (Black Perspex 962, Plasticstocktist, UK). Every batch was incubated in a closed shaker (Certomat® BS1, Sartorius Stedim Biotech, Germany) at 30±1°C under dark conditions and at 37±1 °C under light conditions: these differences in temperature were due to an uncontrolled heat derived from the lamps. The flasks were kept under agitation at 170 rpm. The cultures were fed with 10 g COD L^{-1} of either glucose or acetate.

Continuous culture conditions

A 2.5-L reactor with 2 L of working volume connected to a controller system (In-Control and Power units, Applikon, Netherlands) was used to tune the syntrophy of FCB and PPB under continuous conditions. The pH was set at 7.0 and regulated with NaOH at 0.25 mol L^{-1} and HCl 1 mol L^{-1} and the temperature was maintained at 30°C with a heat exchanger.

The reactor was irradiated from two opposite sides with 2 incandescent lights filtered for wavelengths $\lambda > 700$ nm by two sheets (Black Perspex 962, Plasticstocktist, UK) to promote PPB growth. The light intensity on the reactor wall was 270 W m^{-2} and was measured with a pyranometer (CMP3, Kipp & Zonen, The Netherlands).

After start-up under batch mode and PPB enrichment with acetate, the dilution rate was set at 0.04 h^{-1}, equal to less than half of the μ_{max} of the PPB representative genus *Rhodopseudomonas* (0.1 h^{-1}) (Cerruti et al., 2020).

Four combinations of energy patterns and carbon sources were tested: (*i*) continuous light with acetate, (*ii*) continuous light with glucose, (*iii*) light/ dark (16/8 h) cycles with acetate, and (*iv*) light/ dark (16/8 h) cycles with glucose. Light and dark alternation was controlled with an automatic switch time controlled (GAMMA, The Netherlands).

After 3 months of continuous cultivation, the carbon source feed was stopped, while phosphate and nitrogen sources were maintained for a period of 4 days (ca 4.5 HRTs), in order to evaluate the hypothesis that PPB can grow on fermentation products produced by FCB.

Mass spectrometry for off-gas analyses

The off-gas of all CSTR was connected to a mass spectrometer (Thermofisher, Prima BT Benchtop MS) which was used to measure the production rates of CO_2 and H_2.

Sampling

All samples were collected in 2 ml Eppendorf tubes, centrifuged at 10000 x *g* for 3 minutes. The biomass pellet was separated from the supernatant and stored at -20°C until further analysis. The supernatant was filtered with 0.2 µm filters (Whatman, US), and stored at -20°C until further analysis. In the batch cultures, the samples were collected every 24 h. During the CSTR, 5 to 9 samples were collected for each condition.

Biomass determination

Biomass concentrations were measured over the time course of the batch and continuous reactors by spectrophotometry (Biochrom, Libra S11, US) absorbance at 660 nm (A_{660}). A calibration curve was

established to correlate A_{660} to g volatile suspended solids (gVSS) concentration: c(gVSS L^{-1}) = 0.61 A_{660}. Biomass gVSS was measured taking samples from the liquid phase, filtering them using 0.2 µm filters (Whatman, 435 USA) and drying the wet filters in a 105 °C stove for 24 h. The filters were then incinerated at 550 °C for 2 h, and weighted.

Amplicon sequencing

DNA was extracted from 0.5-7 mg biomass using DNeasy Powersoil microbial extraction kit (Qiagen, Hilden, Germany) accordingly to manufacturer's instructions and stored at -20°C. The compositions of the bacterial communities of the mixed liquors were characterized from the samples collected by V3-V4 16S rRNA gene-based amplicon sequencing as in (Cerruti, Stevens, et al., 2020). The fastq files provided from Novogene were analysed with QIIME2 pipeline (Bolyen et al., 2019).

Chromatography analysis of substrate conversions and fermentation products

Substrate depletion (acetate and glucose) and fermentation products formation (succinate, propionate, formate, lactate, acetate, butyrate) and were scanned and monitored using high-performance liquid chromatography (HPLC) (Waters, 2707, NL) equipped with an Aminex HPX-87H column (BioRad, USA) column. The eluent used was H_3PO_4 (1.5 mmol L^{-1}) at a flowrate of 0.6 mL min^{-1} and at a temperature of 60°C. The compounds were detected by refraction index (Waters 2414, US) and UV (210 nm, Waters 2489, US). Ethanol was quantified through gas-chromatography as in (Julius L Rombouts et al., 2019a).

Wavelength scans of biomass samples to track PPB

Wavelength scan of biomass samples were done using a spectrophotometer (DR3900, Hach, Germany) in order to evaluate the presence of the typical PPB photopigments (carotenoids at 400-

500 nm and bacteriochloropyll at ca 850 nm). Absorbance profiles were measured at each wavelength between 320 nm and 999 nm.

Solver for pathway utilization prediction

To evaluate the fractions of metabolic fermentation and phototrophic pathways, a numerical model was set up which could estimate pathway fractions through minimizing the residual sum squared error (SSQ) using Microsoft Excel 16.48, using the following formula:

$$\min(SSQ) = \min\left(\sqrt{\sum_{i=1}^{n} \frac{(\hat{y}_i - y_i)^2}{n}}\right) \quad \text{(eq. 1)}$$

Where $\hat{y}_i$ is the modelled yield value and y_i is the measured yield value, and n is the amount of metabolic compounds that are considered. The estimated yields were calculated using different fractions of metabolic pathways, which could be varied by the solver to minimize the SSQ (**Table 3**). This SSQ value was minimized using the Generalized Reduced Gradient (GRG) Nonlinear solver available in Excel. The pathways that were used varied per enrichment, depending on the microbial community structure, assuming only the activity of relevant catabolic and anabolic pathways. To simulate the batch enrichments the equations 1.1-1.8 were used. To simulate the CSTRs, reactions 1.9-.10 were also added (Table 3). The result of the pathway modelling was used to create **Figure 7**, visualizing in a semi-quantitative way the flux distribution of the different pathways.

Table 3. Putative reactions included in the numerical model of metabolic reactions along FCB and PPB pathways. The reactions 1.1-1.8 were used to evaluate the contribution of each pathway under batch conditions. The reactions 1.9 and 1.10 were included in the simulation of the CSTRs.

Microbial guilds	Pathways	Reactions
FCB	Glucose → Biomass + CO_2	(1.1)
	Glucose → Ethanol + CO_2	(1.2)
	Glucose + H_2O → Acetate + Ethanol + H^+ + H_2 + CO_2	(1.3)
	Glucose → Butyrate + CO_2 + H_2O	(1.4)
	Glucose → Succinate	(1.5)
	Glucose → Lactate + H^+	(1.6)
	Lactate → Acetate + Propionate + CO_2 + H_2O	(1.7)
FCB + PPB	Formate → CO_2 + H_2	(1.8)
PPB	Acetate → Biomass + CO_2	(1.9)
	CO_2 + H_2O → Biomass + H_2	(1.10)

RESULTS & DISCUSSION

The batch and continuous reactor experiments revealed key insights on the microbial community engineering principles governing the selection, competition and interaction between FCB and PPB in function of substrates, light patterns, and reactor regimes.

Batch conditions

In mixed-culture batch mode, PPB were selected on acetate and IR light

Under batch conditions, the acetate-fed cultures grew only when subjected to light, reaching a biomass concentration of 1 gVSS L^{-1} (μ= 0.0411 ± 0.0007 h^{-1}), with a yield of biomass on substrate

of 0.60 ± 0.09 C-mmol$_X$ C-mmol$_S^{-1}$. Little growth was reported in the six days of cultivation for the acetate cultures in the dark, with a biomass specific growth rate (μ) of 0.006 h^{-1}.

The inocula of the batches originated from a PPB in-house enrichment culture operated as SBR in parallel to the experiments. The inoculum seeded in the acetate-fed batches presented a relative abundance above 60% (vs. total amplicon sequencing read counts) of the purple non-sulfur genus *Rhodopseudomonas*. In the acetate-fed batches, *Rhodopseudomonas* sp. reached as high as 80% of the total community after 6 days of cultivation under IR light. Despite the low growth, chemoorganoheterotrophs of the family of the *Moraxellaceae* showed the highest relative abundance (80%) in the dark (**Figure 1A**).

Acetate is one of the preferred substrates for PPB (Blankenship et al., 1995). It is assimilated into biomass by many PPB species, through the tricarboxylic acids cycle (Pechter et al., 2016). Acetate and IR light selected for *Rhodopseudomonas* under acetate/light conditions. Among the PPB, *Rhodopseudomonas* has the highest growth rate on acetate (μ_{max} = 0.15 h^{-1}) (Cerruti, Ouboter, et al., 2020) and therefore was predominant at the end of the batch cultivation. The growth rate in the acetate-fed cultures under dark conditions was 7 times lower than under light conditions, and the biomass concentration after 6 days was 270 times lower than under light conditions. Under dark conditions, acetate can only be assimilated in presence of suitable electron acceptors (such as S^0 or SO_4^{2-}) in order to produce ATP for growth (Madigan et al., 1982). In the batches, little external electron acceptor was present in the medium (3 mmol SO_4^{2-} L^{-1}). This can explain the very low biomass growth under dark conditions compared to the light one.

In mixed-culture batch mode, FCB were selected on glucose

In the glucose-fed batches a higher biomass concentration was reached in the dark (1 gVSS L^{-1}) than in the light (0.4 gVSS L^{-1}), with a specific μ of 0.070 ± 0.001 h^{-1} and 0.020 ± 0.002 h^{-1} respectively.

The inoculum of glucose-fed batches was dominated by the purple sulfur genus *Thiobaca*, due to microbial community variations in the parent reactor. In the glucose batch cultivation, the genus of *Enterobacter* was predominant, above 90% of the total sequencing reads (**Figure 1A**), both under light and dark conditions. The pH was not controlled in batch cultivations: in the glucose-fed batches pH dropped to 4 within 48 h, despite the presence of the HEPES buffer (**Figure 1B**).

The *Enterobacteriaceae* family is known to be predominant in anaerobic environment in presence of non-limiting concentration of monomeric carbohydrates, such as glucose (de Vrije & Claassen, 2003) (de Vrije & Claassen, 2003). Rombouts et al., 2019 reported an enrichment of 75% of the genus *Enterobacter* in a glucose-fed SBR, in nutrient, temperature and pH conditions similar to the one here presented.

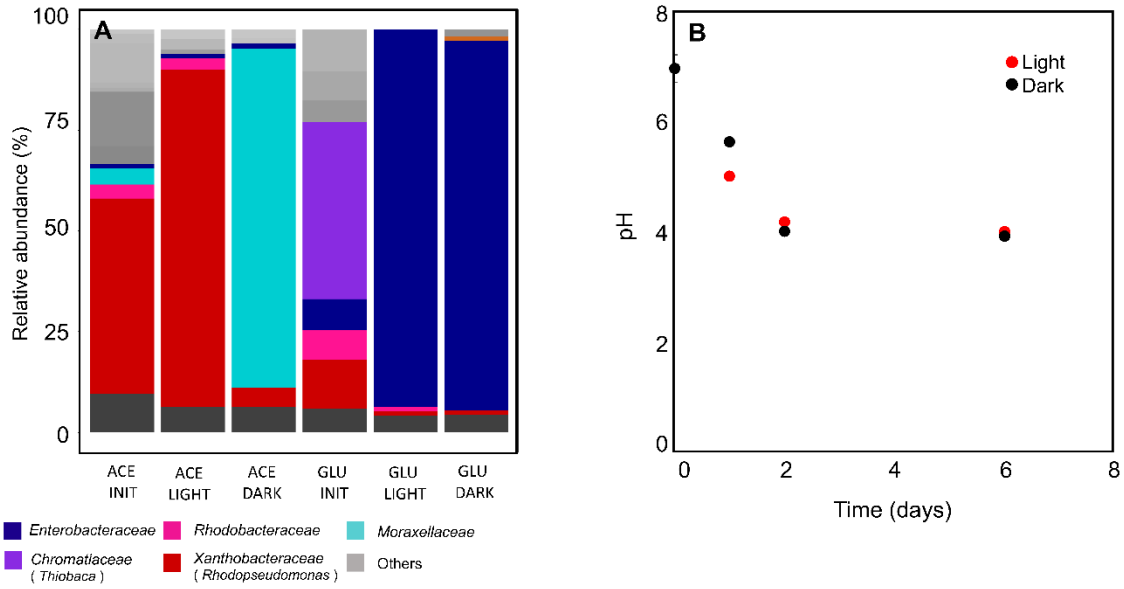

Figure 1. A: Microbial community composition in batches. PPB are dominant at the beginning of the cultivation (ACE INIT and GLU INIT). After 6 days of cultivation under acetate feed, PPB were dominant under light conditions (ACE LIGHT). Under acetate-dark conditions there was little grow from the genus *Moraxellaceae*. Under glucose feed, independently of the light conditions, the genus Enterobacteriaceae was dominant. **B:** pH evolution in the glucose-fed batches. Both under light and under dark conditions the pH dropped to 4 in the first 2 days of incubation.

Ethanol was the main fermentation product under glucose-fed batch conditions

Under acetate-fed batch conditions in the light, acetate was fully depleted after 6 days of incubation. Under glucose-fed batch conditions the biomass yield over glucose were 0.052 ± 0.002 C-mmol$_X$ C-mmol$_S^{-1}$ and 0.134 ± 0.011 C-mmol$_X$ C-mmol$_S^{-1}$ under light and under dark conditions respectively. After six days of cultivation, in the glucose-fed batches in the dark, ethanol was the main fermentation product, with a yield of 0.20 ± 0.10 C-mmol$_{et}$ C-mmol$_S^{-1}$, followed by succinate (0.07 ± 0.03 C-mmol$_{succ}$ C-mmol$_S^{-1}$) and acetate (0.03 ± 0.01 C-mmol$_{ace}$ C-mmol$_S^{-1}$). In the glucose-fed batches under light conditions, after 6 days of cultivation 30% of the initial glucose was still present in the reaction broth, and carbon balances could not be properly closed (>90% recovery). Ethanol was the main fermentation product (0.10 ± 0.07 C-mmol$_{et}$ C-mmol$_S^{-1}$), followed by lactate (0.05 C-mmol$_{lac}$ C-mmol$_S^{-1}$) and succinate (0.04 ± 0.02 C-mmol$_{succ}$ C-mmol$_S^{-1}$).

A solver enabled to evaluate the theoretical contribution of 8 putative fermentation pathways to the overall carbon and electron balances. Under batch conditions the phototrophic pathways were not included in the simulation, as PPB relative abundance was very low as measured by amplicon sequencing (~1%) (**Figure 1A**). The predicted contribution of the singular pathways to the overall yields of the batches under light and dark conditions were comparable. Under batch conditions, the dominant metabolic pathway was identified as homo-ethanol production form glucose (**Table 3**, Eq. 1.2). This catabolism is associated with the fermentative *Enterobacteriaceae* (Jang et al., 2017).

Wavelength scan is commonly used as an indirect measure for the presence of PPB in the cultures (Fiedor et al., 2016), as photopigments absorb photons with specific wavelengths. Absorbance peaks around 400-500 nm represent the carotenoids series, and the peaks around 850 nm the bacteriochlorophyll a (Stomp et al., 2007). In the acetate-based batches in the light the aforementioned peaks were clearly detected at 450 nm and 800-850 nm. In the acetate-fed batches in

304 the dark, almost no growth was reported in the 6 days incubation and peak for photopigments was
305 detected at 800 and 850 nm. In the glucose-fed batches, both dark and light, no peaks were observed
306 (**Figure 2A/B**). These results suggested the selective growth of PPB in illuminated acetate batches,
307 and of non-phototrophic organisms in the glucose-batches.

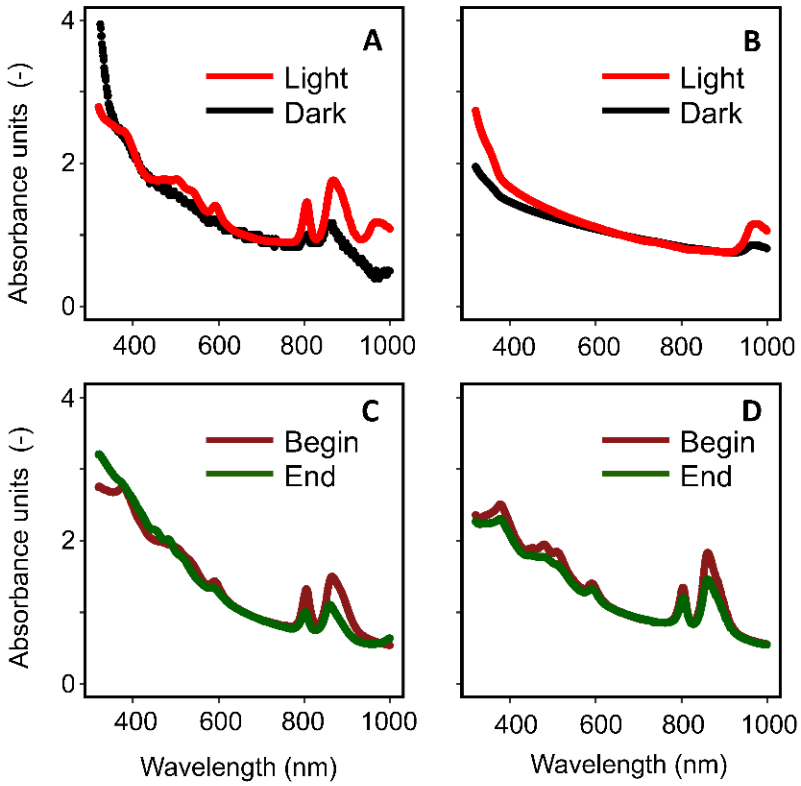

308

309 **Figure 2.** Wavelength scan from 300 to 1000 nm. Absorbance units normalized for the biomass concentration (as A.U.
310 at 660nm). **A:** acetate-fed batches. The typical PPB peaks (at ca 850 nm) were clearly visible under light conditions. **B:**
311 glucose-fed batches. No peak was present. **C:** continuous light glucose-fed CSTR. The presence of PPB was confirmed
312 by the presence of their typical peaks. **D:** dark / light glucose-fed CSTR. The presence of PPB was confirmed by the
313 presence of their typical peaks.

314

315 ***Enterobacteriaceae were enriched due to higher growth rates***

316 The maximum biomass specific growth rate (μ_{max}) is a key factor driving selection mechanisms in
317 substrate-rich environments (Winkler et al., 2017), if no significant intermediate storage of substrate

is displayed. FCB-like species of the genus *Enterobacter* present a μ_{max} of 0.45 – 0.80 h^{-1} in mineral medium conditions with low sugar concentrations (<10 g_{COD} L^{-1}) (Füchslin et al., 2012; Rombouts et al., 2019). When fermenting carbohydrates like glucose, *Rhodopseudomonas capsulata* grows at a μ_{max} of 0.014 h^{-1} (Conrad & Schlegel, 1978). In batches, where the substrate is not limiting, the organisms with higher uptakes rates will be selected above organisms with high biomass yields (Rombouts et al 2019). According to the Herbert-Pirt relation, when the substrate uptake is directly coupled with growth, the organisms with the highest growth rate dominate. Using these studies, the genus *Enterobacter* is estimated to have a μ_{max} about 32 times higher than *Rhodopseudomonas* under glucose feed, making it successful in the competition for glucose in batch.

Under batch conditions, both in the light and in the dark, the family of the *Enterobacteriaceae* was enriched (>90%). The species belonging to the family of the *Enterobacteriaceae* ferment sugars through either the Embden-Meyerhof pathway or the pentose phosphate pathway, with a net production of ethanol (Jang et al., 2017). Ethanol can be used as substrate for growth by PPB, but with a strict pH regulation (pH = 7) (Inui et al., 1995).

Due to lactate production, which is a major byproduct of ethanol fermentation (Converti & Perego, 2002), and insufficient pH buffer, the pH dropped to 4 within the first 2 days of cultivation, as the pK_a of lactic acid is 3.8 (**Figure 1B**). Fermentative bacteria can still grow at low pH (pH < 5.5) (Tsuji et al., 1982). PPB grow instead in a pH range between 6.5 and 9.0, with an optimum at 7.0 (Pfennig, 1977). The low pH (pH = 4) resulting from the glucose-fed batch experiments could have prevented the PPB to uptake and grow on the alcohols and VFAs produced by *Enterobacter*, leading to a low relative abundance (~ 1%) in the glucose-fed batches. We postulate that with a strict pH control to 7, PPB will be able to grow on fermentation products of *Enterobacteriaceae*.

The genus *Enterobacter* can grow in a range of temperature between 20 and 45°C (Gill & Suisted, 1978), with an optimum growth temperature at 40°C (Tanisho, 1998). The temperature differences

here reported for glucose-fed batches under dark and light (ca. 7°C difference) should not have affected its specific growth rates. On the other hand, light has been used as a control method for fermentative organism proliferation (D'Ercole et al., 2016; Gwynne & Gallagher, 2018). As IR light was provided to the illuminated cultures, we postulate its inhibitory action on the *Enterobacteriaceae* family, resulting in lower growth rates (3.5 times lower) compared to the dark cultures. How this inhibition by photons actually works on cellular and molecular level remains to be settled by future work.

Continuous culture

Under continuous-flow regime, four different light and substrate conditions were imposed (1- acetate under light, 2- acetate under light / dark cycles, 3- glucose under light, and 4- glucose under light and dark cycles). The pH was controlled at 7.0 to favor the enrichment of PPB.

CO_2 production rate increased with an increased biomass growth

The CO_2 partial pressure in the off-gas of the CSTR was monitored to evaluate the growth state of the biomass. For PPB, CO_2 production is a side product of acetate assimilation (Sadaie et al., 1997). In acetate-fed CSTRs, CO_2 production was constant under continuous illumination (0.0111 ± 0.0004 $C\text{-}mmol_{CO2}$ $C\text{-}mmol_S^{-1}$) (**Figure 3A**). When dark / light cycles were applied, the CO_2 production decreased to 0 C-mmol h^{-1} during the 8 h dark periods and increased again to 0.3 C-mmol h^{-1} during the 16 h light phases (**Figure 3B**). The CO_2 production during the light phases indicated that acetate was continuously assimilated, whereas the sudden decrease during the dark periods (1/3 less within the first hour of dark) indicated that the metabolic activity was switched off. An oscillation in the CO_2 production rate was already observed in *Rhodopseudomonas* pure cultures under CSTR (Cerruti et al., 2020). In both cases, when the substrate was provided in excess, PPB grew with a growth rate close to μ_{max} (0.1 h^{-1}) during the light periods. In the dark, PPB halted their metabolic activity.

Both under continuous illumination and dark/light cycles, a change in CO_2 production was observed 24-48 h after the switch from acetate feed to glucose feed. In the CSTR under continuous illumination, a peak of CO_2 production reached 1.2 C-mmol h^{-1} 24 h (ca 1 HRT) after the switch to the glucose feed and stabilized at 0.6 C-mmol h^{-1} 2 days later (**Figure 3A**). Under light / dark cycles a peak of CO_2 production (up to 5.6 C-mmol h^{-1}) was observed after two full cycles (3.8 HRTs from the glucose switch). After 8 HRTs from the switch to the glucose feed, the CO_2 production rate presented oscillations between light and dark periods. The CO_2 production rate increased of 0.5 C-mmol h^{-1} at the beginning of the light phase and it decreased of 0.4 C-mmol h^{-1} in every dark period (**Figure 3B**). This behavior was observed for 8 HRTs, until the pH dropped to 2 due to a technical failure.

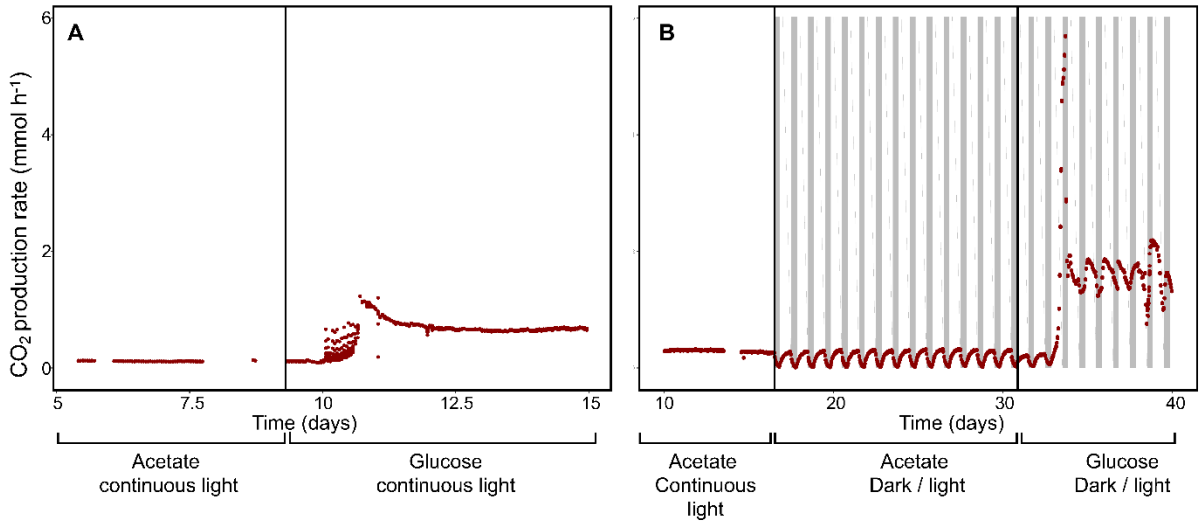

Figure 3. A: CO_2 production rates under acetate-fed and glucose-fed CSTR continuous light conditions. An increase of ca 1 mmol h-1 was observed 3 days after the switch to glucose feed, and then stabilized. **B:** CO_2 production rates under acetate continuous light, acetate dark / light and glucose dark / light conditions. Under acetate continuous illumination CO_2 was produced at constant rate. Under acetate dark / light CO_2 was produced only during the light periods. Under glucose dark / light conditions, a peak in production rate was observed after 3 days from the switch to the glucose-feed. The production rates increased during dark periods and decreased during light periods.

Ethanol was the main fermentation product also in glucose-fed CSTR

Under glucose-fed CSTR conditions, the biomass yield over glucose was 0.22 ± 0.02 C-mmol$_X$ C-mmols^{-1} and 0.45 ± 0.12 C-mmol$_X$ C-mmols^{-1} under continuous illumination and light / dark cycles respectively. Ethanol was the main measured fermentation product (0.18 ± 0.06 and 0.11 ± 0.10 C-mmol$_{et}$ C-mmols^{-1} under continuous light and dark / light cycles respectively). In the CSTR under continuous illumination also acetate was measured (0.21 ± 0.15 C-mmol$_{ace}$ C-mmols^{-1}) and butyrate (0.06 ± 0.05 C-mmol$_{but}$ C-mmols^{-1}). In the CSTR under dark / light cycles, formate (0.11 ± 0.01 C-mmol$_{form}$ C-mmols^{-1}) and butyrate (0.10 ± 0.01 C-mmol$_{but}$ C-mmols^{-1}) were measured (**Figure 4**).

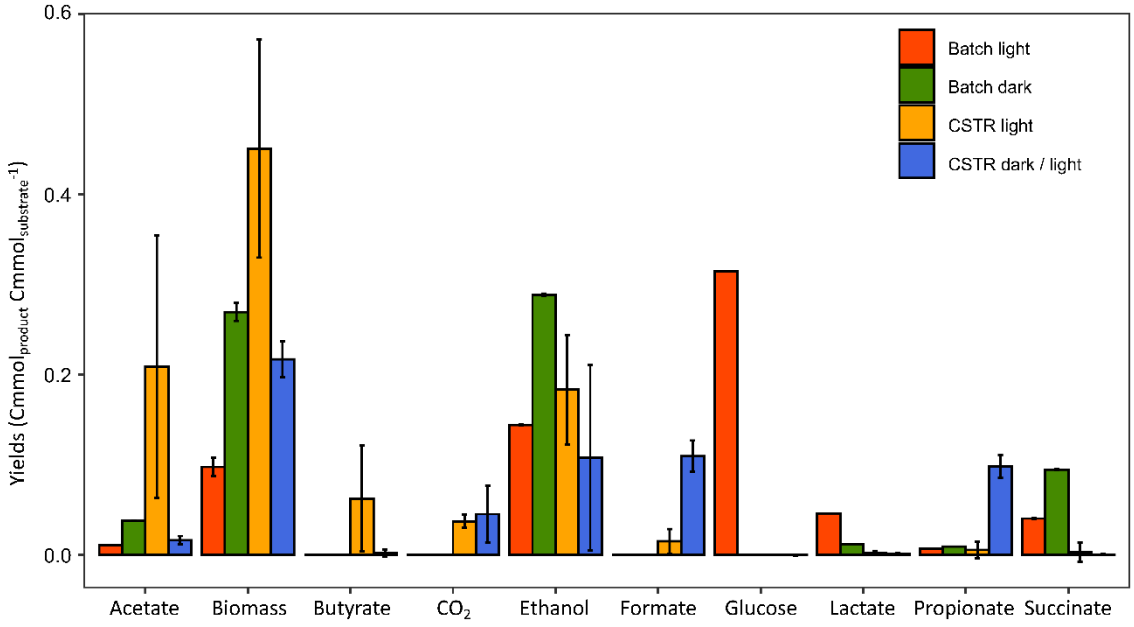

Figure 4. Yields of the glucose-fed cultures. Under batch conditions, the main fermentation products were ethanol and succinate. Under light conditions, glucose was not fully depleted. Under CSTR conditions, the main fermentation products were ethanol, formate and acetate.

Under CSTR conditions, photoautotrophic CO_2 fixation (photosynthesis) and photoheterotrophic acetate assimilation were added to the solver matrix, to evaluate the contribution of PPB to the total carbon and energy balances. Under all CSTR conditions the major fermentation pathway involved

401 the glucose fermentation through the acetyl-CoA pathway (**Figure 5**) (83% and 55% for continuous
402 illumination and dark / light cycles respectively). The solver estimated a high contribution of the
403 photoautotrophic pathway in the CSTR under continuous illumination, and of the photoheterotrophic
404 pathway under dark / light cycles.

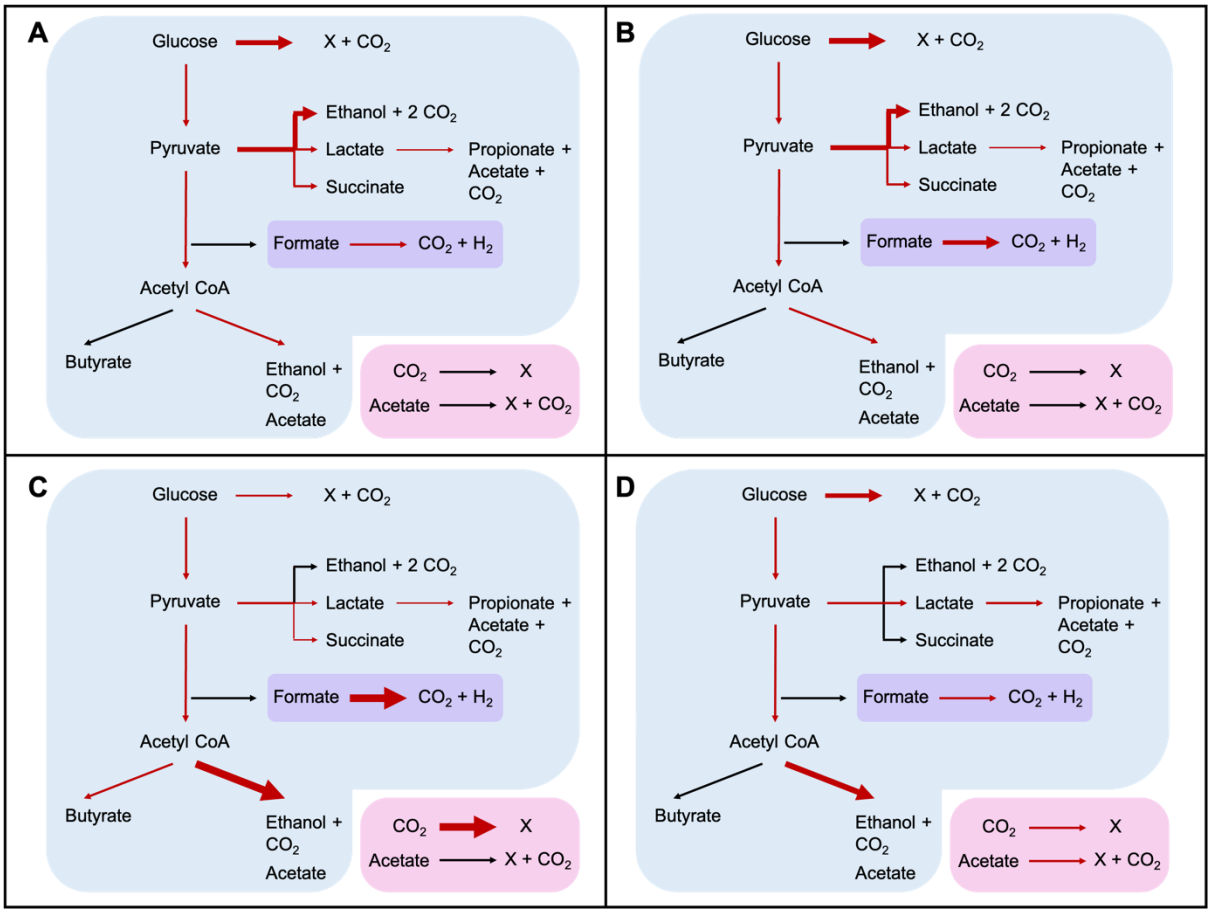

405

406 **Figure 5.** Pathways involved under the different reactor regimes. The thickness of the arrows represents the predicted
407 yield toward a specific metabolic route, based on the calculations of the solver. The reactions with the blue background
408 are performed by FCB. The reaction with the purple background is performed by both FCB and PPB. The reactions with
409 the pink background are performed by PPB. **A:** batch conditions with continuous illumination. **B:** batch conditions in the
410 dark. **C:** CSTR under continuous illumination. **D:** CSTR conditions under light / dark cycles. Under batch conditions the
411 pathways used were mainly directed toward biomass and ethanol production. Under CSTR ethanol was the main
412 fermentation product, but the production of propionate, succinate and lactate was predicted. The phototrophic pathways
413 were not included for the batch conditions but were included in the carbon and electron balance of the CSTRs.

414

PPB were enriched in the acetate-fed CSTR

Under continuous illumination and with acetate as carbon and electron source PPB formed the dominant guild (on average 68 ± 21 %) (**Figure 6**). The genus *Rhodopseudomonas* was predominant at the beginning of the CSTR (65%), while its relative abundance decreased to 40% after one week of cultivation (8.5 HRT). Simultaneously, the genus *Rhodobacter* got enriched (from 13 to 23%). A further enrichment of *Rhodobacter* was observed once the light/dark cycles were applied, reaching around 65% of the total population after 15.6 HRTs, while *Rhodopseudomonas* abundance was stable below 10%.

In the acetate-fed CSTR under continuous light the biomass concentration was not constant. Once the dark / light cycles were applied, the biomass production followed the irradiation pattern. The biomass reached a concentration of 44.75 ± 1.24 C-mmol L^{-1} after the light periods, and it decreased to 37.58 ± 0.09 C-mmol L^{-1} after the dark periods. Under anaerobic conditions, PPB do not grow in the dark in absence of an external electron donor (Madigan et al., 1982; Yen & Marrs, 1977), but growth is restored once the light is present (Cerruti et al., 2020; Zhi et al., 2019). The biomass concentration increased without stabilizing in the light periods, as in (Cerruti et al., 2020). Acetate was not consumed during the dark phases, and its concentration increased due to continuous supply in the CSTR. In a chemostat, the growth rate of the microbial community is defined by the dilution rate and the concentration of the limiting compound, if no biofilm is formed (Kuenen, 2019). An increase in biomass concentration during the illumination times implied that the growth rate of the microorganisms (0.1 h^{-1}) was higher than the dilution rate (0.04 h^{-1}), as a consequence of high residual acetate concentration. During the dark cycles, acetate consumption stopped, acetate accumulated, to be used in light cycles by the PPB organisms. This a higher growth rate than the applied dilution rate, which fits with standard Monod kinetics for growth.

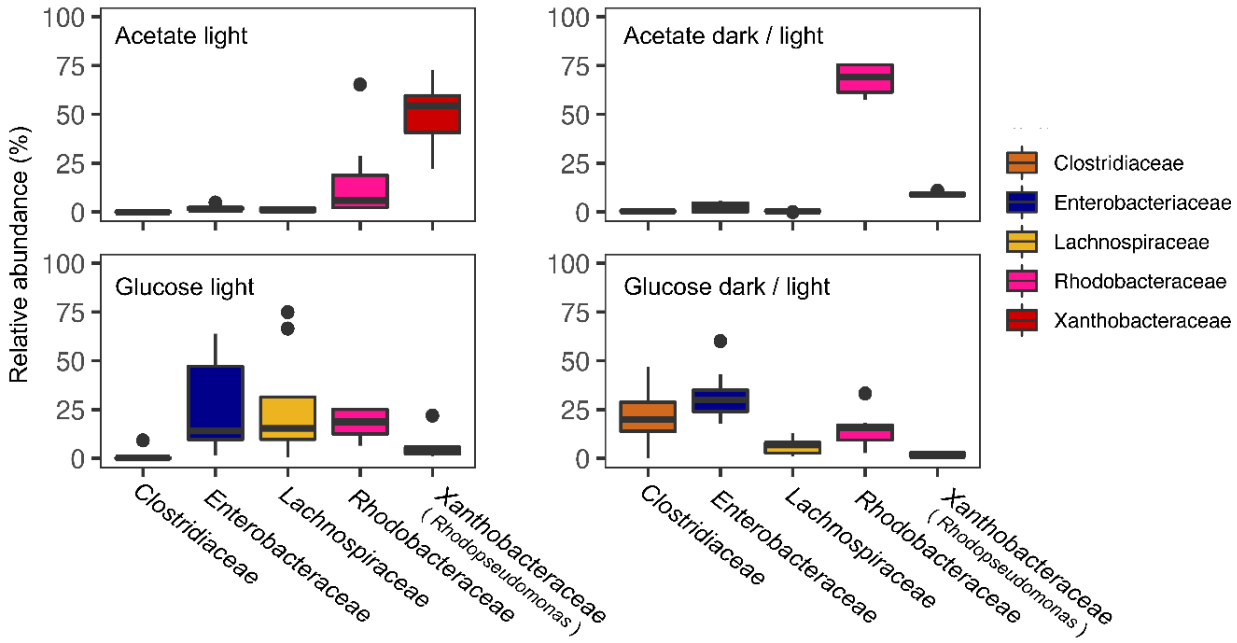

439

440 **Figure 6.** Relative abundance under CSTR conditions. Under acetate conditions, PPB were dominant community, with a
441 shift from *Rhodopseudomonas* under continuous illumination to *Rhodobacter* under light / dark conditions. Under glucose
442 feed, the FCB were dominant, especially the genera *Enterobacteriaceae* and *Lachnospiraceae*.

443

444 ***FCB were enriched in the glucose-fed CSTR***

445 In the CSTR, FCB accounted for more of the 50% of the sequences under glucose feed, regardless
446 the light condition. In CSTR, light and dark cycles had an impact on the selection process of the FCB.
447 Under continuous illumination, the family of *Lachnospiraceae* was predominant (around 30 % of the
448 total community, with a peak at 75%), followed by the family of *Enterobacteriaceae* (15%) (**Figure**
449 **6**). Under light/dark cycles *Enterobacteriaceae* was the most predominant (32 ± 17 %), along with
450 *Clostridiaceae* (18 ± 15 %).
451 Among the PPB guild, *Rhodobacter* was the only PPB to significantly persist in the glucose-fed
452 CSTR, with an average relative abundance of 19.5 ± 14 % (**Figure 6**) independently of the light
453 conditions. The persistence of PPB in the glucose-fed CSTRs was further proven by the wavelength

454 scan. Peaks for the bacteriochlorphyll and the carotenoids were identified at 400-450, 800 and 850
455 nm for both the continuous illumination and the light / dark cycles (**Figure 2C/D**).
456
457 ***The microbial community defined the fermentation products production***
458 The families of *Clostridiaceae, Enterobacteri*aceae and *Lachnospiraceae* are able to ferment glucose.
459 They compete for glucose through different fermentation pathways (Grimmler et al., 2011; Horiuchi
460 et al., 2002). *Lachnospiraceae* and *Clostridiaceae* are phylogenetically and morphologically
461 heterogeneous families belonging to the phylum of *Firmicutes* (De Vos et al., 2005). Glucose
462 fermentation through the acetyl-CoA pathway is typical of *Clostridiaceae* (Aristilde et al., 2015). In
463 human gut microbiota, they contribute to sugar fermentation to lactate and short-chain fatty acids
464 production (Venegas et al., 2019). Butyrate was produced only in the CSTR under continuous
465 illumination (0.06 ± 0.05 C-mmol C-mmol$_S^{-1}$). The *Lachnospiraceae* and *Clostridiaceae* families
466 ferment glucose into primarily butyrate, acetate and ethanol (Rombouts et al., 2019b; Temudo et al.,
467 2008; Valk et al., 2018). Butyrate is produced through the butyril-CoA dehydrogenase gene,
468 responsible for the conversion of crotonyl-CoA to butyryl-CoA and the butyryl-CoA:acetyl-CoA
469 transferase (Venegas et al., 2019). According to the NCBI database (NCBI, 2021), the gene encoding
470 for this enzyme is present in the phylum of *Firmicutes* that comprises *Clostridiaceae* and
471 *Lachnospiraceae* relatives, but not in the proteobacterial family of the *Enterobacteriaceae*,
472 explaining the absence of butyrate in the glucose-fed batches.
473 Under dark / light CSTR conditions, the relatively high production of propionate (0.10 ± 0.01 C-
474 mmol C-mmol$_S^{-1}$, 17 times higher than under continuous illumination), can be linked to the
475 abundance of *Clostridiaceae*, which are propionate producers (Johns, 1952). *Clostridium* species can
476 present a μ_{max} of 0.25 h^{-1} (Gomez-Flores et al., 2015) with primary fermentation products including
477 ethanol, butyrate, acetate and propionate (Huang et al., 1986; Lamed et al., 1988). *Clostridium*
478 *beijerincki* has been reported to decrease the H_2 production when exposed to light intensities above

200 W m^{-2}, with a shift from a preferential production of butyric acid to acetic acid (Zagrodnik & Laniecki, 2016). The continuous illumination under CSTR conditions might have resulted in an inhibition of *Clostridiaceae*, with an enrichment of other *Firmicutes* like *Lachnospiraceae*, through an unknown mechanism.

Formate and propionate production was 10 times higher under light/ dark conditions compared to continuous illumination. Acetate production was instead 12 times lower under dark / light cycles compared to the continuous illumination (**Figure 4**). This was probably linked to a higher abundance family of the *Enterobacteriaceae* under dark / light cycles compared to the continuous illumination (31% and 18% respectively) (**Figure 6**). *Enterobacteriaceae* present a μ_{max} 0.5-1 h^{-1} (Khanna et al., 2012; Martens et al., 1999) and are known to ferment sugars to primarily ethanol, with lactate and acetate as major byproduct during ethanol fermentation (Converti & Perego, 2002).

PPB grew on FCB fermentation products

After 3 months of CSTR operation, to test the hypothesis that PPB grow on the fermentation products of FCB, the glucose feed was stopped while nitrogen and phosphate were still provided. Along the 4 days of operation, the relative abundance of the PPB shifted from ca 10 to 50% (**Figure 7A**). The biomass concentration sharply decreased already 2 h after stopping the glucose feed, stabilizing at a concentration of 15.7 ± 2 C-$mmol_X$ L^{-1}. Butyrate, ethanol, formate, lactate, propionate and succinate were washed out of the system at the imposed dilution rate (0.04 h^{-1}). Acetate was depleted in 50 h, 4 times faster than the theoretical washout rate (**Figure 7B**). In absence of glucose as carbon source, the highly active fermentative organisms were not growing. The increase in the PPB relative abundance proved the interaction with FCB, showing that PPB utilize VFAs as preferred substrate and can selectively grow on FCB fermentation products.

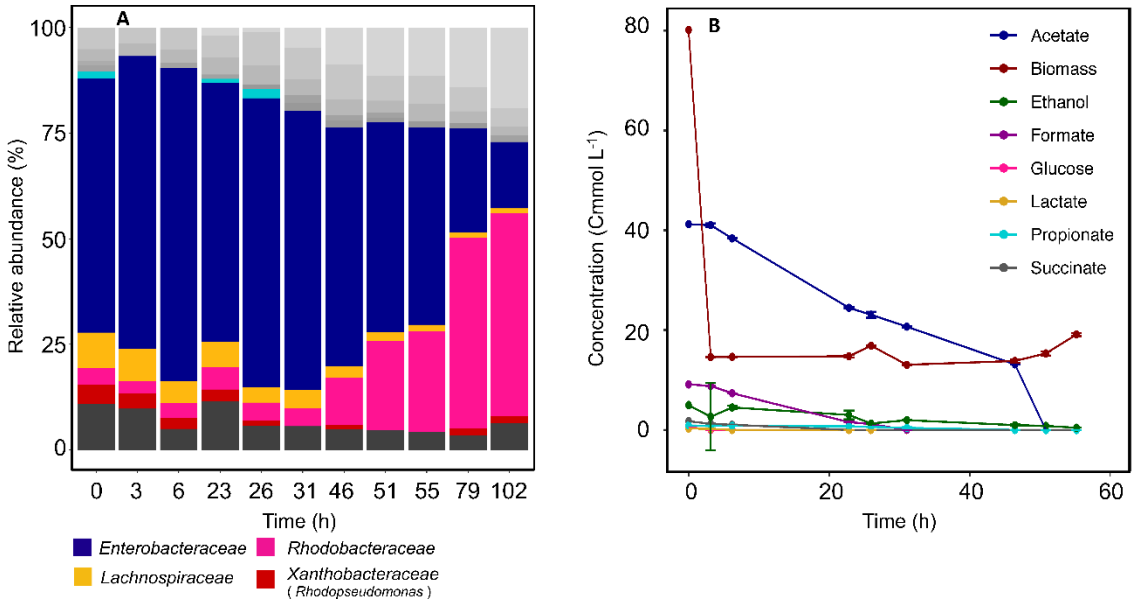

503

504 **Figure 7. A:** Microbial composition after the stop to the glucose feed. Over time, the FCB relative abundance decreased
505 over time, while the *Rhodobacteraceae* increased. **B:** Fermentation products concentration after the glucose feed-stop.
506 After 55 h all the fermentation products were depleted.

507

508 **Outlook**

509

510 ***Metabolic strategies for microbial enrichment***

511 Microorganisms use a combination of adaptive reactions to coexist with other organisms (Panikov,
512 2010). Based on the adaptation techniques, two major types of organisms can be identified (Andrews
513 & Harris, 1986; Cowan et al., 2000): r- and K-strategists. The r-strategists show high growth and
514 conversion rates, in low-populated and resources-rich environments. K-strategists thrive in highly
515 populated environments, where the resources are limited. They exhibit lower growth rates but high
516 substrate conversion yields.
517 Under the different reactor regimes, the microbial communities followed this postulate.
518 *Enterobacteriaceae* were predominant under non-limiting conditions can be classified as r-

519 organisms. *Clostridiaceae* and *Lachnospiraceae* showed high growth rates in nutrient-limiting
520 environments and can be classified as K-strategists. Among the PPB guild, *Rhodopseuodmonas*
521 showed a high-rate behaviour, dominating in substrate-rich environments. *Rhodobacter* showed high
522 efficiency typical of the K-organisms, being able to survive also to nutrient-limited environments, as
523 the CSTRs (**Table 4**).
524
525 **Table 4.** Reported maximum growth rates of the main FCB and PPB in the systems under glucose and acetate feed and
526 adaptation strategies.

Substrates	**Maximum growth rate μ_{max} (h^{-1})**				
	Fermentative chemoorganoheterotrophic bacteria (FCB)			**Purple photoorganoheterotrophic bacteria (PPB)**	
	Enterobacteriaceae	***Lachnospiraceae***	***Clostridiaceae***	***Rhodopseudomonas***	***Rhodobacter***
Glucose	0.3 – 1 (Hasona et al., 2004; Khanna et al., 2012)	0.3 (Soto-Martin et al., 2020)	0.25 (Gomez-Flores et al., 2015)	0.014 (Conrad & Schlegel, 1978)	0.1 (Imam et al., 2011)
Acetate	-	-	-	0.15 (Cerruti et al., 2020)	0.05 (Kopf & Newman, 2012)
Selection strategy	r-strategist (on glucose)	K-strategist (on glucose)	K-strategist (on glucose)	r-strategist (on acetate)	K-strategist (on acetate)

527
528 Kinetic parameters define the microbial selection mechanisms in CSTRs (Kuenen, 2019). In the
529 CSTRs, the dilution rate was relatively low (0.04 h^{-1}) compared to the growth rates of the fermentative
530 organisms (0.5-1 h^{-1}), as it was set to retain PPB in the system. In a continuous culture, the substrate
531 (in this case glucose) is the limiting compound, and the organisms with higher affinity for it will be
532 predominant (Andrews & Harris, 1986). Within the guild of fermentative organisms, *Clostridiaceae*

533 and *Lachnospiaraceae* are expected to have a lower affinity constant (K_s) and therefore have
534 established over *Enterobacteriaceae.* The controlled pH and an appropriate dilution factor (D = 0.04
535 h^{-1}) allowed the persistence of PPB. In particular, *Rhodobacter* was enriched in the glucose-fed
536 CSTRs regardless the illumination conditions. We propose here a syntrophic association of FCB and
537 PPB for glucose conversion toward CO_2 and biomass (**Figure**). Glucose was first converted into
538 acetate, ethanol, formate and lactate, and lactate was further transformed into acetate and propionate.
539 All the fermentation products can be potentially used by PPB for growth.
540
541 ***Syntrophic associations between FCB and PPB***
542 The interaction between fermentative organisms and purple bacteria is an example of syntrophic
543 interaction. Syntrophy has been shown in biofilms and sludges, where a mass transport of compounds
544 occurs between organisms (Rodríguez et al., 2006). Here, we showed the establishment of a metabolic
545 cooperativity that lead to a multispecies consortium, combining sugar degradation with VFAs
546 assimilation. In nature, PPB are present in many aquatic environments where IR light is present, and
547 they have been found also in anthropogenic environments such as WWTPs. They harness their ability
548 to grow on a diverse range of compounds, creating a wide metabolic net of interaction with other
549 organisms.
550
551 The syntrophy between FO and PPB is not only important at an ecological level but can also be
552 exploited for wastewater treatment. The FCB are used to treat food and agricultural wastes, to degrade
553 sugars and produce biofuels as bioethanol and hydrogen gas of VFAs (Li et al., 2015; Thapa et al.,
554 2015, 2019). Further efforts have been put to selectively direct PPB bioproduct formation toward one
555 or another metabolic route (Puyol et al., 2017), with success. PPB, thanks to high biomass yields
556 (Alloul et al., 2018), harbor a major industrial potential for the production of antioxidants and single-

cell proteins. It has been proven that their biomass can be used as feed for shrimps without protein extraction (Qin et al., 2018).

Advantages of single-sludge vs. two-sludge processes for conversions of glucose by FCB and PPB

The single-step bioprocess implemented here has the advantage to simultaneously treat carbohydrate-rich wastewaters, factually removing the organic pollutants, and enriching organisms with high industrial potential, by combining the metabolic properties of FCB and PPB in one single sludge. An integrated single-stage process combining fermentation and purple photoorganoheterotrophy would allow to treat carbohydrate-rich wastewater in only one tank. The illumination conditions did not affect the syntrophy between FCB and PPB. A discontinuous illumination would reduce the operational costs compared to a continuously irradiated system (Qin et al., 2018). Understanding interactions between the FCB and PPB microbial guilds will help design efficient processes for carbohydrates-based wastewater treatment and valorization. If the aim is then to maximize and valorize the PPB biomass, a two-sludge process can be efficient to first ferment carbohydrates in the first tank selecting for FCB and then supplying the fermentation products like VFAs (whose spectrum can be engineered by mastering selection conditions) to the PPB tank.

Conclusions

FCB and PPB interact as syntrophic organisms. FCB degrade glucose into VFAs, lactate and ethanol. Acetate was assimilated into biomass by PPB. The operational conditions are crucial to establish an interaction between the guilds. FCB are more efficient fermenters than PPB (although their metabolic versatility can allow for fermentation). Under glucose-fed batch regime FCB were enriched over PPB. Under glucose-fed CSTR conditions PPB population got enriched up to 30% in syntrophic association

with FCB. An appropriate dilution rate (0.04 h^{-1}) and pH regulation to 7 enabled to enrich PPB in glucose-rich environments by enabling their metabolic coupling with FCB.

ACKNOWLEDGEMENTS

This study was funded by the start-up grant of the TU Delft Department of Biotechnology (Prof. David Weissbrodt). The authors warmly acknowledge Dirk Geerts, Zita van der Krogt and Ben Abbas for their technical assistance in fermentation and molecular biology labs at TU Delft.

CONFLICT OF INTEREST STATEMENT

The authors share no conflict of interest.

REFERENCES

Abo-Hashesh, M., & Hallenbeck, P. C. (2012). Microaerobic dark fermentative hydrogen production by the photosynthetic bacterium, *Rhodobacter capsulatus* JP91. *International Journal of Low-Carbon Technologies*, *7*(2), 97–103. https://doi.org/10.1093/ijlct/cts011

Alloul, A., Ganigué, R., Spiller, M., Meerburg, F., Cagnetta, C., Rabaey, K., & Vlaeminck, S. E. (2018). Capture−Ferment−Upgrade: A Three-Step Approach for the Valorization of Sewage Organics as Commodities. *Environmental Science & Technology*, *52*(12), 6729–6742 https://doi.org/10.1021/acs.est.7b05712

Andrews, J. H., & Harris, R. F. (1986). r- and K-Selection and Microbial Ecology. *Advances in Microbial Ecology* (pp. 99–147). https://doi.org/10.1007/978-1-4757-0611-6_3

Aristilde, L., Lewis, I. A., Park, J. O., & Rabinowitz, J. D. (2015). Hierarchy in pentose sugar metabolism in *Clostridium acetobutyricum*. *Applied and Environmental Microbiology*, *81*(4), 1452–1462. https://doi.org/10.1128/AEM.03199-14

Blankenship, R., Madigan, M., & Bauer, C. (1995). *Anoxygenic Photosynthetic Bacteria* (R. E. Blankenship, M. T. Madigan, & C. E. Bauer (eds.); Vol. 2). *Springer Netherlands*. https://doi.org/10.1007/0-306-47954-0

Bolyen, E., Rideout, J. R., Dillon, M. R., Bokulich, N. A., Abnet, C. C., Al-Ghalith, G. A., Alexander, H., Alm, E. J., Arumugam, M., Asnicar, F., Bai, Y., Bisanz, J. E., Bittinger, K., Brejnrod, A., Brislawn, C. J., Brown, C. T., Callahan, B. J., Caraballo-Rodríguez, A. M., Chase, Caporaso, J. G. (2019). Reproducible, interactive, scalable and extensible microbiome

612 data science using QIIME 2. *Nature Biotechnology* 37(8), 852–857.
613 https://doi.org/10.1038/s41587-019-0209-9

614 Cerruti, M., Ouboter, H. T., Chasna, V., M van Loosdrecht, M. C., & Weissbrodt, D. G. (2020).
615 Effects of light / dark diel cycles on the photoorganoheterotrophic metabolism of
616 *Rhodopseudomonas palustris* for differential electron allocation to PHAs and H_2. *bioRxiv*
617 2020.08.19.258533. https://doi.org/10.1101/2020.08.19.258533

618 Cerruti, M., Stevens, B., Ebrahimi, S., Alloul, A., Vlaeminck, S. E., & Weissbrodt, D. G. (2020).
619 Enriching and aggregating purple non-sulfur bacteria in an anaerobic sequencing-batch
620 photobioreactor for nutrient capture from wastewater. *Frontiers in Bioengineering and*
621 *Biotechnology*, *8*, 1432. https://doi.org/10.1101/2020.01.08.899062

622 Conrad, R., & Schlegel, H. G. (1978). Regulation of Glucose, Fructose and Sucrose Catabolism in
623 Rhodopseudomonas capsulata. *Journal of General Microbiology*, *105*(2), 315–322.
624 https://doi.org/10.1099/00221287-105-2-315

625 Converti, A., & Perego, P. (2002). Use of carbon and energy balances in the study of the anaerobic
626 metabolism of Enterobacter aerogenes at variable starting glucose concentrations. *Applied*
627 *Microbiology and Biotechnology*, *59*(2–3), 303–309. https://doi.org/10.1007/s00253-002-
628 1009-5

629 Cowan, S. E., Gilbert, E., Liepmann, D., Keasling, J. D., Bioengineering Graduate Program, J., &
630 Francisco, S. (2000). Commensal Interactions in a Dual-Species Biofilm Exposed to Mixed
631 Organic Compounds. In *Applied and Environmental Microbiology* (Vol. 66, Issue 10).
632 http://aem.asm.org/

633 D'Ercole, S., Spoto, G., Trentini, P., Tripodi, D., & Petrini, M. (2016). In vitro inactivation of
634 Enterococcus faecalis with a led device. *Journal of Photochemistry and Photobiology B:*
635 *Biology*, *160*, 172–177. https://doi.org/10.1016/j.jphotobiol.2016.04.015

636 De Vos, P., Garrity, G., Jones, D., Krieg, N. R., Ludwig, W., Rainey, F. A., Schleifer, K.-H., &
637 Whitman, W. B. (2005). The Firmicutes. In D. J. Brenner, N. R. Krieg, & J. T. Staley (Eds.),
638 *Bergey's Manual® of Systematic Bacteriology*. Springer US. https://doi.org/10.1007/0-387-
639 29298-5

640 de Vrije, G. J., & Claassen, P. A. M. (2003). Bio-methane & bio-hydrogen : status and perspectives
641 of biological methane and hydrogen production (J. H. Reith & R. H. Wijffels (eds.)). *Dutch*
642 *Biological Hydrogen Foundation.*

643 Füchslin, H. P., Schneider, C., & Egli, T. (2012). In glucose-limited continuous culture the
644 minimum substrate concentration for growth, Smin, is crucial in the competition between the
645 enterobacterium *Escherichia coli* and *Chelatobacter heintzii*, an environmentally abundant
646 bacterium. *The ISME Journal*, *6*(4), 777–789. https://doi.org/10.1038/ismej.2011.143

647 Ghimire, A., Frunzo, L., Pirozzi, F., Trably, E., Escudie, R., Lens, P. N. L., & Esposito, G. (2015).
648 A review on dark fermentative biohydrogen production from organic biomass: Process

parameters and use of by-products. *Applied Energy*, *144*, 73–95. https://doi.org/10.1016/j.apenergy.2015.01.045

Ghosh, S., Dairkee, U. K., Chowdhury, R., & Bhattacharya, P. (2017). Hydrogen from food processing wastes via photofermentation using Purple Non-sulfur Bacteria (PNSB) – A review. *Energy Conversion and Management*, *141*, 299-314. https://doi.org/10.1016/j.enconman.2016.09.001

Gill, C. O., & Suisted, J. R. (1978). The effects of temperature and growth rate on the proportion of unsaturated fatty acids in bacterial lipids. *Journal of General Microbiology*, *104*(1), 31–36. https://doi.org/10.1099/00221287-104-1-31

Gomez-Flores, M., Nakhla, G., & Hafez, H. (2015). Microbial kinetics of Clostridium termitidis on cellobiose and glucose for biohydrogen production. *Biotechnology Letters*, *37*(10), 1965–1971. https://doi.org/10.1007/s10529-015-1891-4

Grimmler, C., Janssen, H., Krauße, D., Fischer, R. J., Bahl, H., Dürre, P., Liebl, W., & Ehrenreich, A. (2011). Genome-wide gene expression analysis of the switch between acidogenesis and solventogenesis in continuous cultures of *Clostridium acetobutylicum*. *Journal of Molecular Microbiology and Biotechnology*, *20*(1), 1–15. https://doi.org/10.1159/000320973

Gwynne, P. J., & Gallagher, M. P. (2018). Light as a Broad-Spectrum Antimicrobial. *Frontiers in Microbiology*, *9*, 119. https://doi.org/10.3389/fmicb.2018.00119

Hasona, A., Kim, Y., Healy, F. G., Ingram, L. O., & Shanmugam, K. T. (2004). Pyruvate Formate Lyase and Acetate Kinase Are Essential for Anaerobic Growth of *Escherichia coli* on Xylose. *Journal of Bacteriology*, *186*(22), 7593–7600. https://doi.org/10.1128/JB.186.22.7593-7600.2004

Horiuchi, J. I., Shimizu, T., Tada, K., Kanno, T., & Kobayashi, M. (2002). Selective production of organic acids in anaerobic acid reactor by pH control. *Bioresource Technology*, *82*(3), 209–213. https://doi.org/10.1016/S0960-8524(01)00195-X

Huang, L. I., Forsberg, C. W., & Gibbins, L. N. (1986). Influence of External pH and Fermentation Products on *Clostridium acetobutylicum* Intracellular pH and Cellular Distribution of Fermentation Products. *Applied and Environmental Microbiology*, *51*(6), 1230-4. https://doi.org/10.1128/aem.51.6.1230-1234.1986

Hunter, C. N., Beatty, F. D., Thurnauer, M. C., & Thomas, J. (2009). The Purple Phototrophic Bacteria. Springer Netherlands. 1013 pp. https://doi.org/10.1007/978-1-4020-8815-5

Imam, S., Yilmaz, S., Sohmen, U., Gorzalski, A. S., Reed, J. L., Noguera, D. R., & Donohue, T. J. (2011). IRsp1095: A genome-scale reconstruction of the *Rhodobacter sphaeroides* metabolic network. *BMC Systems Biology*, *5*(July). https://doi.org/10.1186/1752-0509-5-116

Inui, M., Momma, K., Matoba, R., Ikuta, M., Yamagata, H., & Yukawa, H. (1995). Characterization of alcohol-assimilating photosynthetic purple non-sulfur bacteria and cloning

of molecular chaperones from a purple non-sulfur bacterium. *Energy Conversion and Management*, *36*(6–9), 767–770. https://doi.org/10.1016/0196-8904(95)00117-V

Jang, J. W., Jung, H. M., Im, D. K., Jung, M. Y., & Oh, M. K. (2017). Pathway engineering of *Enterobacter aerogenes* to improve acetoin production by reducing by-products formation. *Enzyme and Microbial Technology*, *106*, 114–118. https://doi.org/10.1016/j.enzmictec.2017.07.009

Johns, A. T. (1952). The Mechanism of Propionic Acid Formation by *Clostridium propionicum*. *Journal of General Microbiology*, *6*(1–2), 123–127. https://doi.org/10.1099/00221287-6-1-2-123

Khanna, N., Kumar, K., Todi, S., & Das, D. (2012). Characteristics of cured and wild strains of *Enterobacter cloacae* IIT-BT 08 for the improvement of biohydrogen production. *International Journal of Hydrogen Energy*, *37*(16), 11666–11676. https://doi.org/10.1016/j.ijhydene.2012.05.051

Kleerebezem, R., & van Loosdrecht, M. C. (2007). Mixed culture biotechnology for bioenergy production. *Current Opinion in Biotechnology*, *18*(3), 207–212. https://doi.org/10.1016/j.copbio.2007.05.001

Kopf, S. H., & Newman, D. K. (2012). Photomixotrophic growth of *Rhodobacter capsulatus* SB1003 on ferrous iron. *Geobiology*, *10*(3), 216–222. https://doi.org/10.1111/j.1472-4669.2011.00313.x

Kuenen, G. J. (2019). Continuous cultures (chemostats). In *Encyclopedia of Microbiology* (pp. 743–761). Elsevier. https://doi.org/10.1016/B978-0-12-801238-3.02490-9

Lamed, R. J., Lobos, J. H., & Su, T. M. (1988). Effects of Stirring and Hydrogen on Fermentation Products of *Clostridium thermocellum*. *Applied and Environmental Microbiology*, *54*(5), 1216–1221. https://doi.org/10.1128/aem.54.5.1216-1221.1988

Li, L., Li, K., Wang, Y., Chen, C., Xu, Y., Zhang, L., Han, B., Gao, C., Tao, F., Ma, C., & Xu, P. (2015). Metabolic engineering of *Enterobacter cloacae* for high-yield production of enantiopure (2R,3R)-2,3-butanediol from lignocellulose-derived sugars. *Metabolic Engineering*, *28*, 19–27. https://doi.org/10.1016/j.ymben.2014.11.010

Madigan, M., Cox, J. C., & Gest, H. (1982). Photopigments in *Rhodopseudomonas capsulata* cells grown anaerobically in darkness. *Journal of Bacteriology*, *150*(3), 1422–1429. https://doi.org/10.1128/JB.150.3.1422-1429.1982

Martens, D. E., Béal, C., Malakar, P., Zwietering, M. H., & Van'T Riet, K. (1999). Modelling the interactions between *Lactobacillus curvatus* and *Enterobacter cloacae*: I. Individual growth kinetics. *International Journal of Food Microbiology*, *51*(1), 53–65. https://doi.org/10.1016/S0168-1605(99)00095-1

NCBI. (n.d.). *Gene [Internet]. Bethesda (MD): National Library of Medicine (US), National Center*

for Biotechnology Information; 2004 – [cited 2021 05 13]. Available from: https://www.ncbi.nlm.nih.gov/gene/No Title.

Okubo, Y., Futamata, H., & Hiraishi, A. (2005). Distribution and Capacity for Utilization of Lower Fatty Acids of Phototrophic Purple Nonsulfur Bacteria in Wastewater Environments. *Microbes and Environments*, *20*(3), 135–143. https://doi.org/10.1264/jsme2.20.135

Panikov, N. S. (2010). Microbial Ecology. In L. K. Wang, V. Ivanov, & J.-H. Tay (Eds.), *Environmental Biotechnology* (pp. 121–191). Humana Press. https://doi.org/10.1007/978-1-60327-140-0_4

Pearman, P. B., Guisan, A., Broennimann, O., & Randin, C. F. (2008). Niche dynamics in space and time. *Trends in Ecology and Evolution*, *23*(3), 149–158. https://doi.org/10.1016/j.tree.2007.11.005

Pechter, K. B., Gallagher, L., Pyles, H., Manoil, C. S., & Harwood, C. S. (2016). Essential genome of the metabolically versatile alphaproteobacterium *Rhodopseudomonas palustris*. *Journal of Bacteriology*, *198*(5), 867-76. https://doi.org/10.1128/JB.00771-15

Pfennig, N. (1977). Phototrophic green and purple bacteria: a comparative, systematic survey. *Annual review of microbiology*, *31*, 275–290. https://doi.org/10.1146/annurev.mi.31.100177.001423

Puyol, D., Barry, E. M., Hülsen, T., & Batstone, D. J. (2017). A mechanistic model for anaerobic phototrophs in domestic wastewater applications: Photo-anaerobic model (PAnM). *Water Research*, *116*, 241–253. https://doi.org/10.1016/j.watres.2017.03.022

Puyol, Daniel, & Batstone, D. J. (2017). Editorial: Resource Recovery from Wastewater by Biological Technologies. *Frontiers in Microbiology*, *8*, 998. https://doi.org/10.3389/fmicb.2017.00998

Qin, C., Lei, Y., & Wu, J. (2018). Light/dark cycle enhancement and energy consumption of tubular microalgal photobioreactors with discrete double inclined ribs. *Bioresources and Bioprocessing*, *5*(1). https://doi.org/10.1186/s40643-018-0214-8

Rai, P. K., & Singh, S. P. (2016). Integrated dark- and photo-fermentation: Recent advances and provisions for improvement. *International Journal of Hydrogen Energy*, *41*(44), 19957–19971. https://doi.org/10.1016/j.ijhydene.2016.08.084

Rodríguez, J., Kleerebezem, R., Lema, J. M., & Van Loosdrecht, M. C. M. (2006). Modeling product formation in anaerobic mixed culture fermentations. *Biotechnology and Bioengineering*, *93*(3), 592–606. https://doi.org/10.1002/bit.20765

Rombouts, Julius L, Mos, G., Weissbrodt, D. G., Kleerebezem, R., & Van Loosdrecht, M. C. M. (2019a). Diversity and metabolism of xylose and glucose fermenting microbial communities in sequencing batch or continuous culturing. *FEMS Microbiology Ecology*, *95*(2), 233. https://doi.org/10.1093/femsec/fiy233

Rombouts, Julius L, Mos, G., Weissbrodt, D. G., Kleerebezem, R., & Van Loosdrecht, M. C. M. (2019b). The impact of mixtures of xylose and glucose on the microbial diversity and fermentative metabolism of sequencing-batch or continuous enrichment cultures. *FEMS Microbiology Ecology*, *95*, 112. https://doi.org/10.1093/femsec/fiz112

Rombouts, Julius Laurens, Kranendonk, E. M. M., Regueira, A., Weissbrodt, D. G., Kleerebezem, R., & Loosdrecht, M. C. M. (2020). Selecting for lactic acid producing and utilising bacteria in anaerobic enrichment cultures. *Biotechnology and Bioengineering*, *117*(5), 1281–1293. https://doi.org/10.1002/bit.27301

Sadaie, M., Nagano, T., Suzuki, T., Shinoyama, H., & Fujii, T. (1997). Some Properties and Physiological Roles of Phosphoenolpyruvate Carboxylase in *Rhodopseudomonas* sp. No. 7 Grown on Ethanol under Anaerobic-light Conditions. *Bioscience, Biotechnology and Biochemistry*, *61*(4), 625–630. https://doi.org/10.1271/bbb.61.625

Soto-Martin, E. C., Warnke, I., Farquharson, F. M., Christodoulou, M., Horgan, G., Derrien, M., Faurie, J.-M., Flint, H. J., Duncan, S. H., & Louis, P. (2020). Vitamin Biosynthesis by Human Gut Butyrate-Producing Bacteria and Cross-Feeding in Synthetic Microbial Communities. *mBio*, *11*(4), e00886-20. https://doi.org/10.1128/mBio.00886-20

Steindler, L., Rubin-Blum, M., Lavy, A., Deines, P., Hammerschmidt, K., & Bosch, T. C. G. (2020). Exploring the Niche Concept in a Simple Metaorganism. *Frontiers in Microbiology*, *11*, 1942. https://doi.org/10.3389/fmicb.2020.01942

Stomp, M., Huisman, J., Stal, L. J., & Matthijs, H. C. P. (2007). Colorful niches of phototrophic microorganisms shaped by vibrations of the water molecule. *The ISME Journal*, *1*(4), 271–282. https://doi.org/10.1038/ismej.2007.59

Tanisho, S. (1998). Hydrogen Production by Facultative Anaerobe Enterobacter aerogenes. In O. R. Zaborsky, J. R. Benemann, T. Matsunaga, J. Miyake, & A. San Pietro (Eds.), *BioHydrogen* (pp. 273–279). Springer US. https://doi.org/10.1007/978-0-585-35132-2_35

Temudo, M. F., Muyzer, G., Kleerebezem, R., & Van Loosdrecht, M. C. M. (2008). Diversity of microbial communities in open mixed culture fermentations: Impact of the pH and carbon source. *Applied Microbiology and Biotechnology*, *80*(6), 1121–1130. https://doi.org/10.1007/s00253-008-1669-x

Thapa, L. P., Lee, S. J., Park, C., & Kim, S. W. (2019). Metabolic engineering of *Enterobacter aerogenes* to improve the production of 2,3-butanediol. *Biochemical Engineering Journal*, *143*, 169–178. https://doi.org/10.1016/j.bej.2018.12.019

Thapa, L. P., Lee, S. J., Yang, X., Lee, J. H., Choi, H. S., Park, C., & Kim, S. W. (2015). Improved bioethanol production from metabolic engineering of *Enterobacter aerogenes* ATCC 29007. *Process Biochemistry*, *50*(12), 2051–2060. https://doi.org/10.1016/j.procbio.2015.09.007

Tsuji, A., Kaneko, Y., Takahashi, K., Ogawa, M., & Goto, S. (1982). The Effects of Temperature and pH on the Growth of Eight Enteric and Nine Glucose Non-Fermenting Species of Gram-

794 Negative Rods. *Microbiology and Immunology*, *26*(1),15-24. https://doi.org/10.1111/j.1348-
795 0421.1982.tb00149.x

796 Valk, L. C., Frank, J., de la Torre-Cortés, P., van 't Hof, M., van Maris, A. J. A., Pronk, J. T., & van
797 Loosdrecht, M. C. M. (2018). Galacturonate metabolism in anaerobic chemostat enrichment
798 cultures: Combined fermentation and acetogenesis by the dominant sp. nov. "*Candidatus*
799 Galacturonibacter soehngenii." *Applied and Environmental Microbiology*, *84*(18), e01370-18.
800 https://doi.org/10.1128/AEM.01370-18

801 Venegas, D. P., De La Fuente, M. K., Landskron, G., González, M. J., Quera, R., Dijkstra, G.,
802 Harmsen, H. J. M., Faber, K. N., & Hermoso, M. A. (2019). Short chain fatty acids (SCFAs)
803 mediated gut epithelial and immune regulation and its relevance for inflammatory bowel
804 diseases. *Frontiers in Immunology*, *10*, 277. https://doi.org/10.3389/fimmu.2019.00277

805 Winkler, M.-K. H., Boets, P., Hahne, B., Goethals, P., & Volcke, E. I. P. (2017). Effect of the
806 dilution rate on microbial competition: r-strategist can win over k-strategist at low substrate
807 concentration. *PLOS One*, *12*(3), e0172785. https://doi.org/10.1371/journal.pone.0172785

808 Yen, H. C., & Marrs, B. (1977). Growth of *Rhodopseudomonas capsulata* under anaerobic dark
809 conditions with dimethyl sulfoxide. *Archives of Biochemistry and Biophysics*, *181*(2), 411–
810 418. https://doi.org/10.1016/0003-9861(77)90246-6

811 Zagrodnik, R., & Laniecki, M. (2016). An unexpected negative influence of light intensity on
812 hydrogen production by dark fermentative bacteria *Clostridium beijerinckii*. *Bioresource*
813 *Technology*, *200*, 1039–1043. https://doi.org/10.1016/j.biortech.2015.10.049

814 Zhi, R., Yang, A., Zhang, G., Zhu, Y., Meng, F., & Li, X. (2019). Effects of light-dark cycles on
815 photosynthetic bacteria wastewater treatment and valuable substances production. *Bioresource*
816 *Technology*, *274*, 496–501. https://doi.org/10.1016/j.biortech.2018.12.021

817

818